

## Electronic Supporting Information

### Facile method to stabilize sodium metal anodes towards high-performance sodium batteries

Qiongqiong Lu,<sup>\*ab</sup> Ahmad Omar,<sup>a</sup> Ling Ding,<sup>ab</sup> Steffen Oswald,<sup>a</sup> Martin Hantusch,<sup>a</sup> Lars Giebel, <sup>a</sup> Cornelius Nielsch<sup>abc</sup> and Daria Mikhailova <sup>\*a</sup>

<sup>a</sup>*Leibniz Institute for Solid State and Materials Research (IFW) Dresden e.V., Helmholtzstraße 20, 01069 Dresden, Germany. E-Mail: q.lu@ifw-dresden.de; d.mikhailova@ifw-dresden.de*

<sup>b</sup>*Institute of Materials Science, Technische Universität Dresden, Helmholtzstraße 7, 01062 Dresden, Germany.*

<sup>c</sup>*Institute of Applied Physics, Technische Universität Dresden, Nöthnitzer Straße 61, 01062 Dresden, Germany*

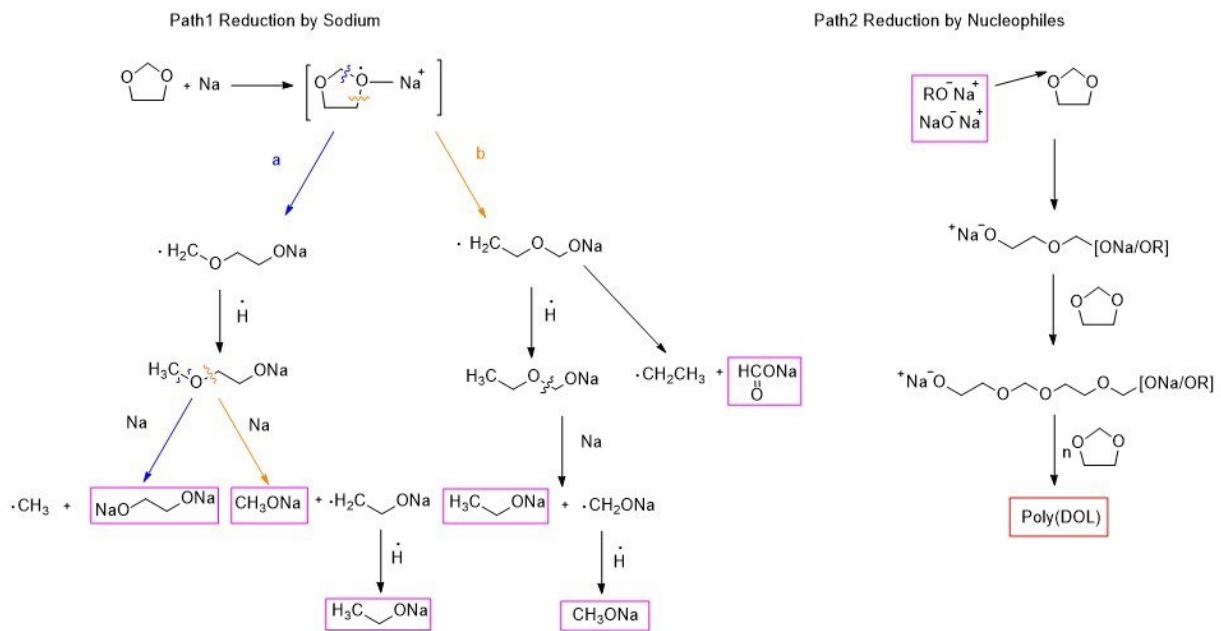


**Fig. S1** Proposed reaction mechanism between DOL and Na, analogously as for the reaction between DOL and Li, according to literature<sup>1</sup>. DOL is the source of  $H_2$ .

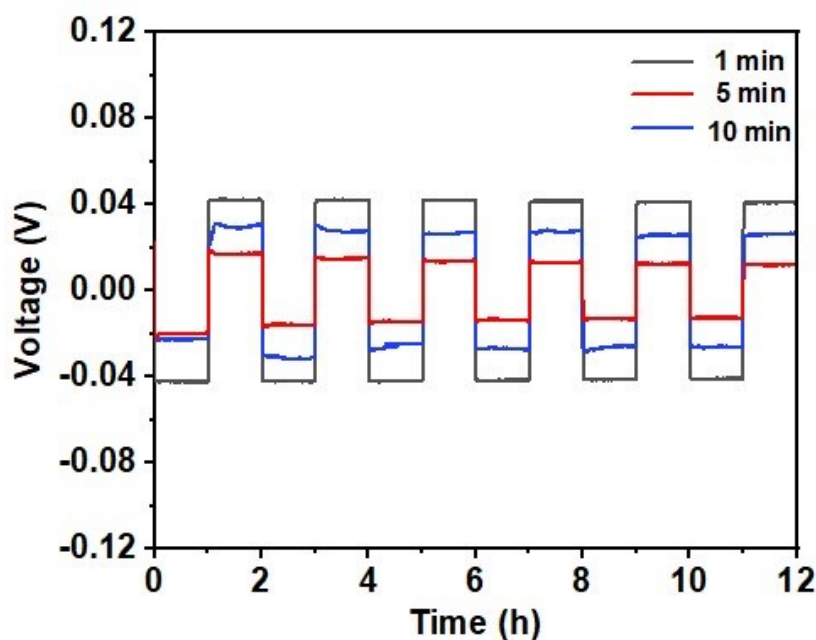
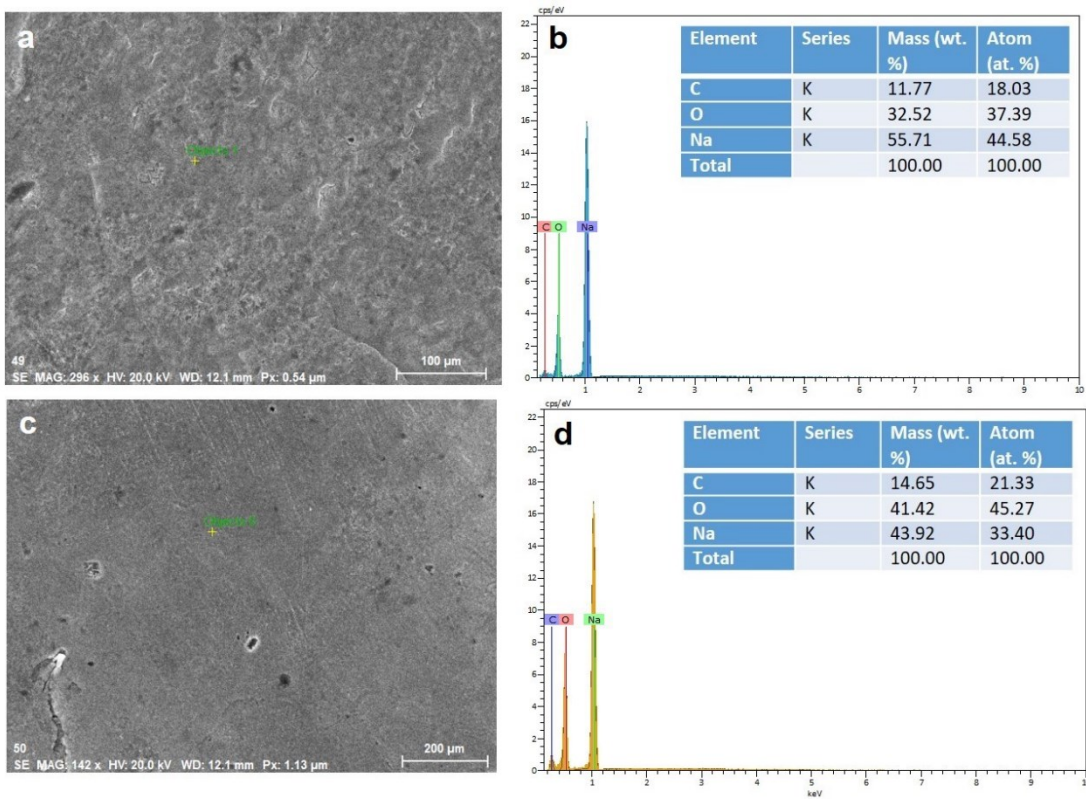


Fig S2. Voltage profiles of symmetric cells of protected Na with different treatment times at current density of 1 mA cm<sup>-2</sup> with a capacity of 1 mAh cm<sup>-2</sup>.



**Fig. S3** SEM images of (a) untreated Na and (c) protected Na. EDXS data of (b) untreated Na and (d) protected Na at selected spot.

**Table S1** Atom concentration table of untreated Na and protected Na measured by XPS, recalculated from both Al source and

Sample	Element	C	O	Na
Untreated Na	Atom concentration (%)	15.3	43.3	41.4
Protected Na	Atom concentration (%)	26.5	43.6	29.8

Mg source.

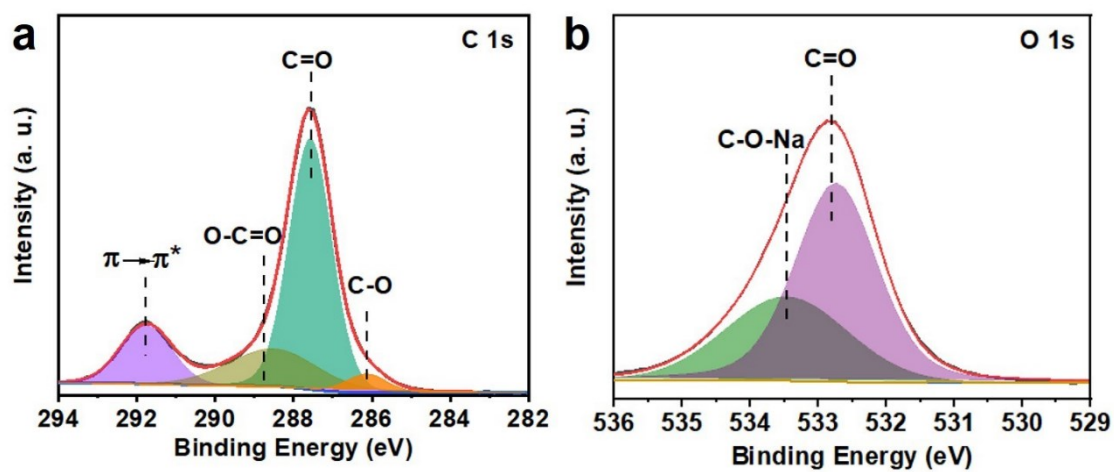


**Fig. S4** High resolution XP spectra of (a) C 1s and (b) O 1s of untreated Na, measured with Al source and Mg source, respectively.

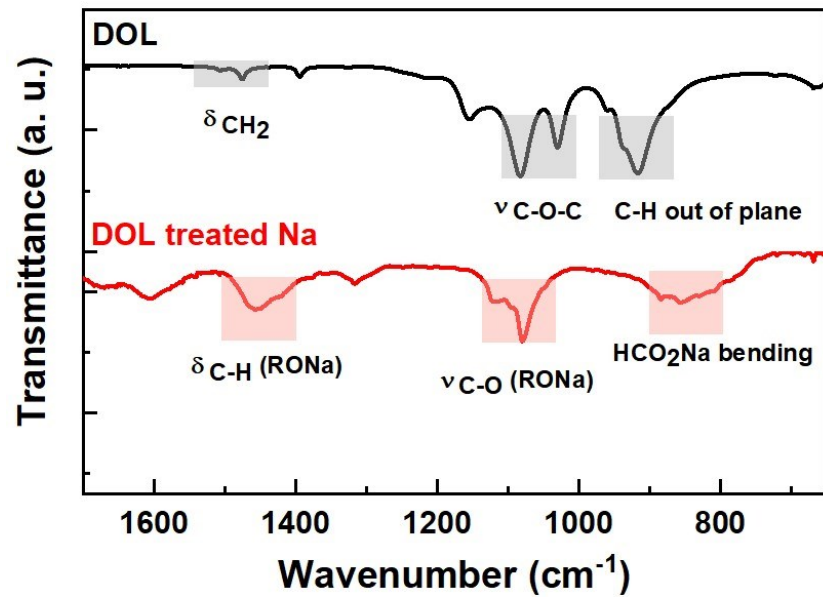


**Fig. S5** FTIR spectra of DOL and Na treated by DOL.

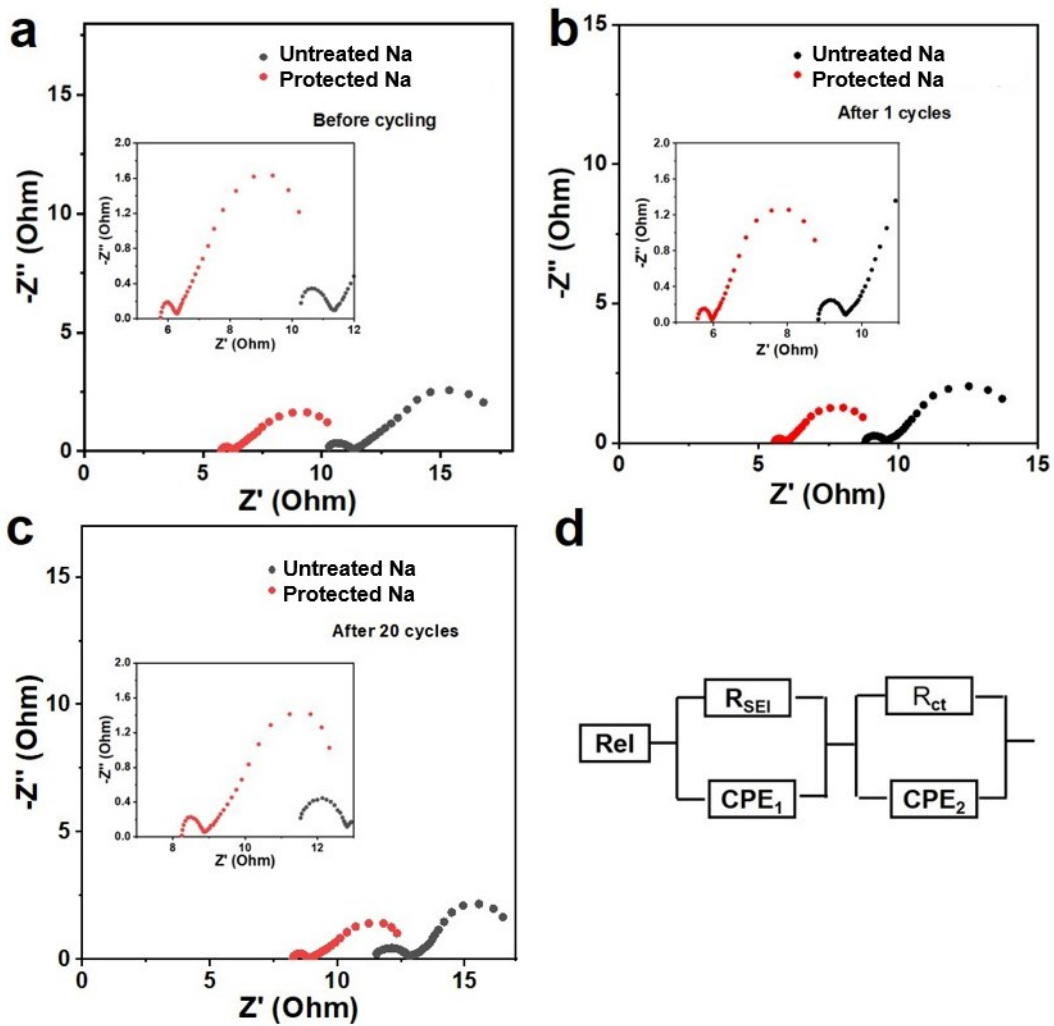


**Fig. S6** Nyquist plots of untreated Na and Na with protective layer (a) before cycle, (b) after 1cycle and (c) after 20 cycles (inset: magnification of Nyquist plot). d) Equivalent circuit model for fitting the Nyquist plots. Here,  $R_{el}$  represents the ion transport in the bulk electrolyte.  $R_{SEI}$  represents interfacial resistance associated with the solid electrolyte interphase between electrode and electrolyte.  $R_{ct}$  denotes the electronic transport in the interface. CPE1 and CPE2 represent the constant phase elements.

**Table S2**  $R_{SEI}$  and  $R_{ct}$  value of untreated Na and protected Na at different stages of cycling.

	Before cycling		After 1 cycle		After 20 cycles	
	$R_{SEI}$ ( $\Omega$ )	$R_{ct}$ ( $\Omega$ )	$R_{SEI}$ ( $\Omega$ )	$R_{ct}$ ( $\Omega$ )	$R_{SEI}$ ( $\Omega$ )	$R_{ct}$ ( $\Omega$ )
Untreated Na	0.93	4.95	0.65	4.05	1.13	4.01
Protected Na	0.45	3.37	0.46	2.59	0.73	2.97

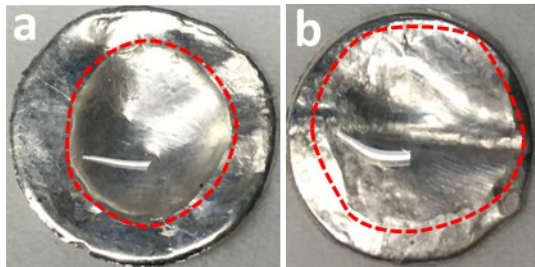


**Fig. S7** Electrolyte wettability of (a) untreated Na and (b) protected Na by adding 30  $\mu\text{L}$  electrolyte on surface of Na electrodes with a diameter of 12 mm in the glovebox. Red dashed line marks the boundary of the electrolyte drop. Due to the high sensitivity of Na metal towards moisture from air, unfortunately it was not possible to perform contact angle tests outside the glovebox. Therefore, we performed this alternative experiment to check the electrolyte wettability.

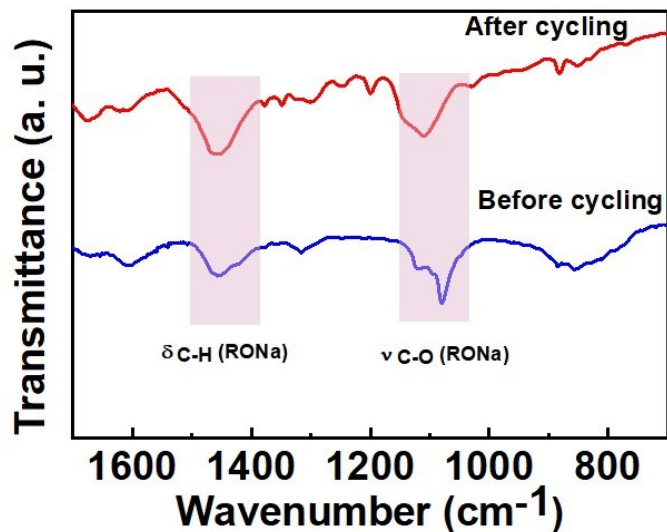


**Fig. S8** FTIR spectra of protected Na and after 20 cycles at a current density of 2  $\text{mA cm}^{-2}$  with a capacity of 1  $\text{mA h cm}^{-2}$ .

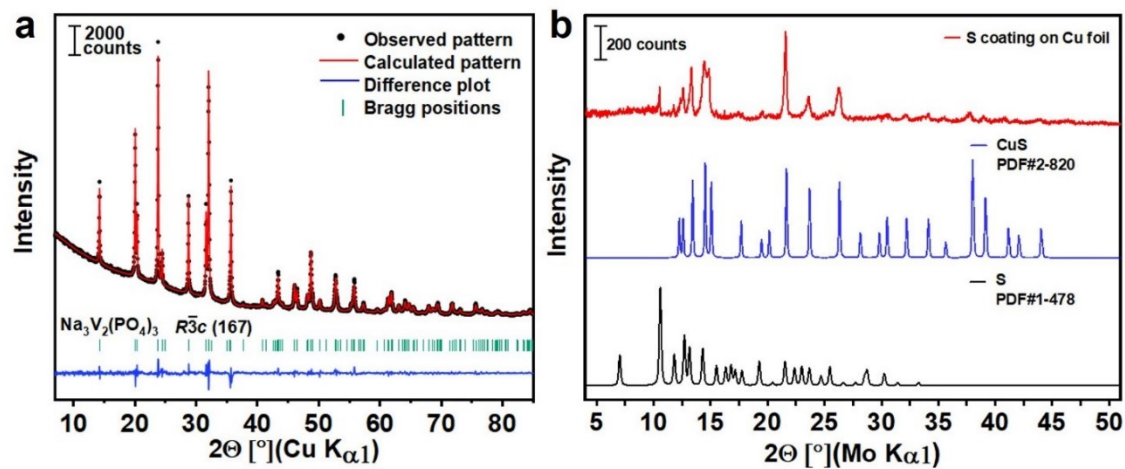


**Fig. S9** (a) XRD pattern of NVP powder with calculated patterns from the Rietveld analysis. (b) XRD pattern of S electrode.

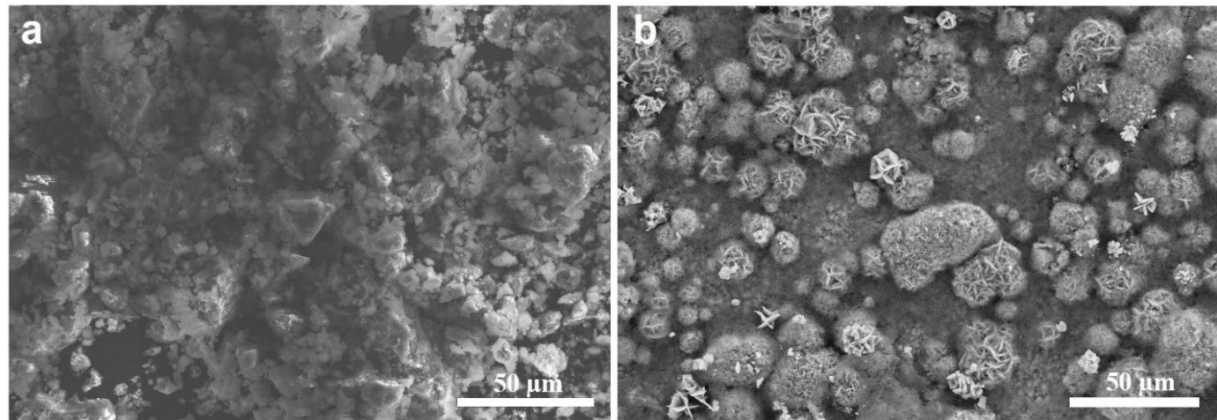


**Fig. S10** SEM images of (a) NVP powder and (b) S electrode.

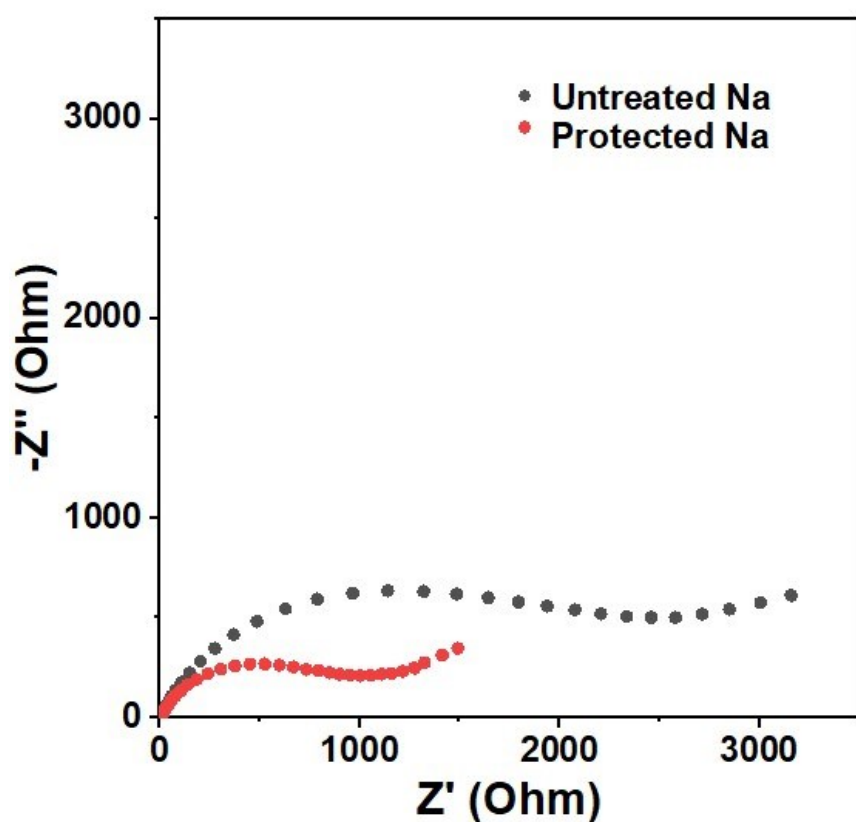


**Fig. S11** Nyquist plot of U-Na//NVP and P-Na//NVP batteries before cycling.

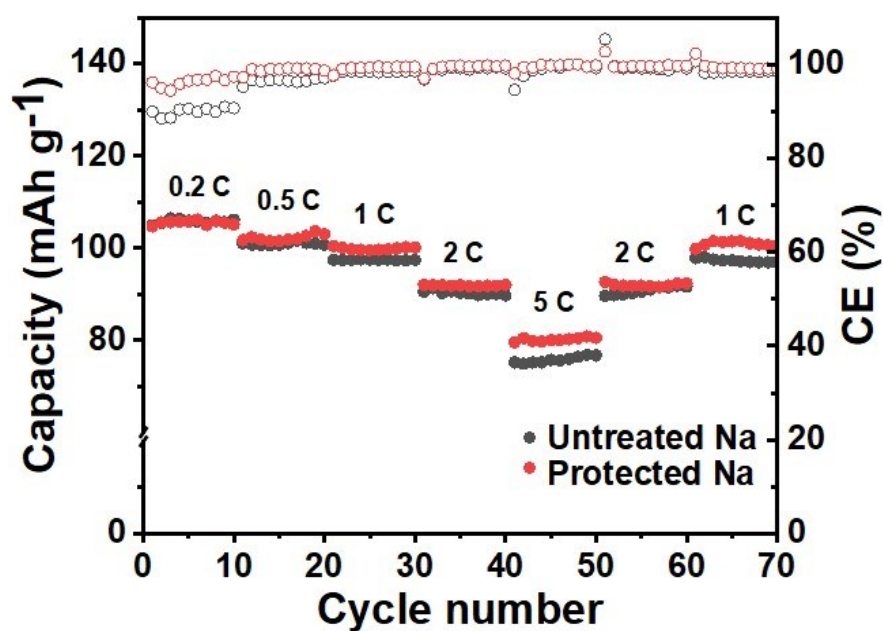


**Fig. S12** Rate performance of Na// $\text{Na}_3\text{V}_2(\text{PO}_4)_3$  and P-Na// $\text{Na}_3\text{V}_2(\text{PO}_4)_3$  batteries.

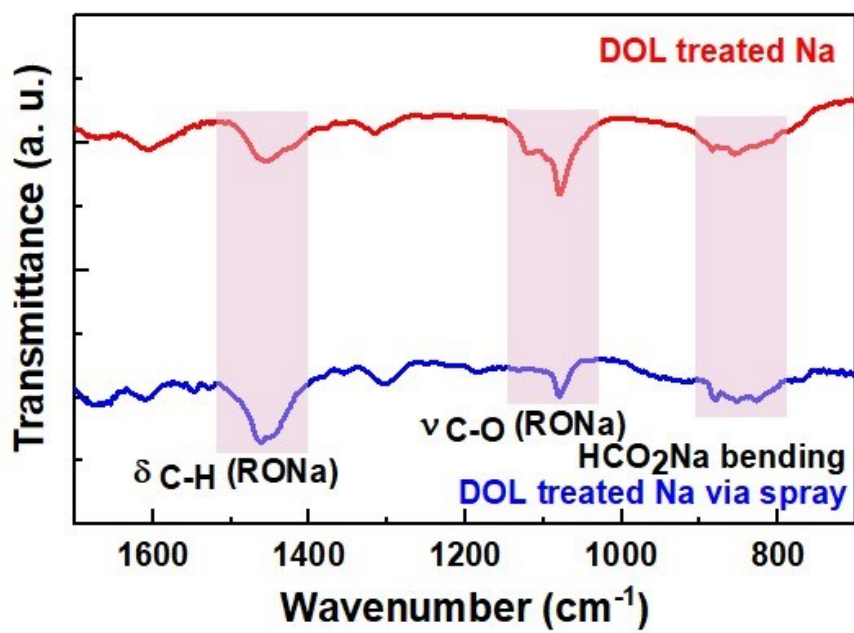


**Fig. S13** IR spectral of protected Na via soaking and protected Na via spray coating.

**Table S3** Comparison of recent literature reports on sodium metal anodes with different protective layers.

Protective layers	Current density / mA cm <sup>-2</sup> Areal capacity / mAh cm <sup>-2</sup>	Overpotential / mV Cycle / h	Reference
Poly(DOL) coating	1, 1	~25, 2800	This work
Bi by treatment	Bi(SO <sub>3</sub> GF <sub>3</sub> ) <sub>3</sub> 0.5, 1	~25, 1000	Batteries & Supercaps 2 (2019) 663–667. <sup>3</sup>
Na-Sn /NaCl by treatment	0.5, 1	~50, 500	J. Phys. Chem. Lett. 10 (2019) 707–714. <sup>4</sup>
Nal layer by iodopropane treatment	0.25, 0.75	60, 500	Nano Energy 57 (2019) 692–702. <sup>5</sup>
N/S co-doped carbon nanotube paper	1, 1	70, 500	Adv. Mater. 30 (2018) 1801334. <sup>6</sup>
NaF by fluoroethylene carbonate treatment	0.15, 0.075	100, 250	Adv. Funct. Mater. 28 (2018) 1706374. <sup>7</sup>
NaBr by 1-bromo-propane treatment	1, 1	~150, 250	Nat. Commun. 8 (2017) 898. <sup>8</sup>
Ultra-thin graphene	1, 1	~250, 200	Nano Lett. 17 (2017) 6808–6815. <sup>9</sup>
Al <sub>2</sub> O <sub>3</sub> layer by plasma-enhanced atomic layer deposition	0.25, 0.062	~70, 450	Adv. Energy Mater. 7 (2017) 1601526. <sup>10</sup>
Al <sub>2</sub> O <sub>3</sub> layer by atomic layer deposition	3, 1	~20, 500	Adv. Mater. 29 (2017) 1606663. <sup>11</sup>
Al <sub>2</sub> O <sub>3</sub> layer by molecular layer deposition	1, 1	300, 270	Nano Lett. 17 (2017) 5653–5659. <sup>12</sup>
Al <sub>2</sub> O <sub>3</sub> layer by blade casting	0.5, 1	1000, 550	ACS Appl. Mater. Interfaces. 9 (2017) 6000–6006. <sup>13</sup>
1-methyl-3-propylimidazolium-chlorate/SiO <sub>2</sub> nanoparticles	1, 1	~35, 40	Adv. Mater. 29 (2017) 1605512. <sup>14</sup>
MoS <sub>2</sub> layer	0.2, 0.2	25, 1000	ACS Appl. Mater. Interfaces. 9 (2017) 40265–40272. <sup>15</sup>

## References

- 1 D. Aurbach, O. Youngman, Y. Gofer and A. Meitav, *Electrochim. Acta*, 1990, **35**, 625-638.
- 2 D. Aurbach, E. Pollak, R. Elazari, G. Salitra, C. S. Kelley and J. Affinito, *J. Electrochem. Soc.*, 2009, **156**, A694-A702.
- 3 M. Ma, Y. Lu, Z. Yan and J. Chen, *Batteries & Supercaps*, 2019, **2**, 663-667.
- 4 X. Zheng, H. Fu, C. Hu, H. Xu, Y. Huang, J. Wen, H. Sun, W. Luo and Y. Huang, *J. Phys. Chem. Lett.*, 2019, **10**, 707-714.
- 5 H. Tian, H. Shao, Y. Chen, X. Fang, P. Xiong, B. Sun, P. H. L. Notten and G. Wang, *Nano Energy*, 2019, **57**, 692-702.
- 6 B. Sun, P. Li, J. Zhang, D. Wang, P. Munroe, C. Wang, P. H. L. Notten and G. Wang, *Adv. Mater.*, 2018, **30**, 1801334.
- 7 S. Wu, Y. Qiao, K. Jiang, Y. He, S. Guo and H. Zhou, *Adv. Funct. Mater.*, 2018, **28**, 1706374.
- 8 S. Choudhury, S. Wei, Y. Ozhabes, D. Gunceler, M. J. Zachman, Z. Tu, J. H. Shin, P. Nath, A. Agrawal, L. F. Kourkoutis, T. A. Arias and L. A. Archer, *Nat. Commun.*, 2017, **8**, 898.
- 9 H. Wang, C. Wang, E. Matios and W. Li, *Nano Lett.*, 2017, **17**, 6808-6815.
- 10 W. Luo, C.-F. Lin, O. Zhao, M. Noked, Y. Zhang, G. W. Rubloff and L. Hu, *Adv. Energy Mater.*, 2017, **7**, 1601526.
- 11 Y. Zhao, L. V. Goncharova, A. Lushington, Q. Sun, H. Yadegari, B. Wang, W. Xiao, R. Li and X. Sun, *Adv. Mater.*, 2017, **29**, 1606663.
- 12 Y. Zhao, L. V. Goncharova, Q. Zhang, P. Kaghazchi, Q. Sun, A. Lushington, B. Wang, R. Li and X. Sun, *Nano Lett.*, 2017, **17**, 5653-5659.
- 13 Y.-J. Kim, H. Lee, H. Noh, J. Lee, S. Kim, M.-H. Ryou, Y. M. Lee and H.-T. Kim, *ACS Appl. Mater. Interfaces*, 2017, **9**, 6000-6006.
- 14 S. Wei, S. Choudhury, J. Xu, P. Nath, Z. Tu and L. A. Archer, *Adv. Mater.*, 2017, **29**, 1605512.
- 15 D. Zhang, B. Li, S. Wang and S. Yang, *ACS Appl. Mater. Interfaces*, 2017, **9**, 40265-40272.